DOI: 10.1002/zaac.201000368

Three New cpt-Metal Complexes Displaying 0D, 1D, and 3D Topology Structures

Jiang-Feng Song,*[a] Rui-Sha Zhou,[a] Jia Zhang,[a] Chun-Yan Xu,[a] Yan-Bing Li,[a] and Biao-Bing Wang[b]

Keywords: 4-(4-Carboxyphenyl)-1,2,4-triazole; Coordination modes; X-ray diffraction; Fluorescence; Solvothermal synthesis

Abstract. Three new cpt-metal complexes of different topology structures were synthesized by solvothermal methods [Hcpt = 4-(4-carboxyphenyl)-1,2,4-triazole]. The structure of $[Mn(cpt)_2 \cdot 2H_2O]$ (**1**) is essentially 0D monomeric, but extended into a 2D supramolecular network through cross-linking hydrogen bonds. In $[Cu(cpt)(OH) \cdot 2H_2O] \cdot 2H_2O$ (**2**), the hydroxo groups as well as cpt ligands join the copper ions into an infinite polymeric [Cu(μ-cpt)(μ-OH)] chain, which is interconnected into a 3D supramolecular network with different oriented channels by 1D water chains. The complex $[Zn(cpt)_2] \cdot 0.5DMF \cdot CH_3CH_2OH$ (**3**), which crystallizes in a 3D open framework with fourfold interpenetrated diamondoid network topology, represents the first 3D structure based on cpt anions. The structure differences demonstrate that the reaction metal ions have an important effect on the structures of these complexes.

Introduction

The interest in metal-organic frameworks (MOF) is rapidly increasing because of their intriguing structures and wide potential applications as functional materials.[1–11] Promising results were achieved and startling applications are being developed, however, the rational design and synthesis of coordination polymers with unique structure and function still remain a long-term challenge. The self-assembly process of coordination polymer is frequently influenced by various factors such as medium, the nature of the organic ligands, pH value of solution, temperature, the nature of metal ions, coordination arrangement, stereochemistry, and number of coordination donors provided by organic ligands.[12–18] Among them, the nature of the organic ligand has a large impact on the building of coordination polymers with novel structures. So, it is important to choose a suitable organic linker that can be much more effective to design metal-organic frameworks.

The choice of 4-(4-carboxyphenyl)-1,2,4-triazole (Hcpt) is based on following considerations: (1) the difference of the asymmetrical coordination sites based on the carboxyl and triazolyl functional group, which easily results in the formation of different topologies, (2) a rigid backbone, which is helpful to construct a stable metal-organic framework, (3) the rotation around the C–C bond among the triazolyl ring, the benzene ring, and the carboxyl group will improve the coordination modes of Hcpt ligand, and (4) a bidentate-bridging coordination mode similar to the 1,2,4-triazole ring results in the short distance of metal–metal.[19–22] Taking all these factors into consideration, we believe that Hcpt will be an ideal ligand for constructing novel metal-organic hybrid complexes.

In 2005, *Guo* reported the first 0D monomeric cobalt complex of Hcpt, in which only one nitrogen atom of triazole ring of cpt^- was involved in the coordination to the cobalt atom.[23] Three 0D isomorphous monomeric complexes (with copper, cadmium, and cobalt) based on the ligand Hcpt were reported by *Lukashuk* et al. in 2007, in which only the carboxylate oxygen atoms of cpt^- were involved in the coordination with the metal atom.[24] Recently, three 0D isomorphous lanthanide complexes with cubane-shaped moieties were reported, in which a new coordination mode of cpt^- was found.[25] The aforementioned results show that investigations on the coordination chemistry of Hcpt are still in their early stages and more systematic research is needed in order to get a better understanding of its coordination abilities.

The present study investigated the effect of the reaction metal ions on the formation of different topology structures constructed by Hcpt ligand. Herein we report the synthesis and the crystal structures of three new coordination complexes $[Mn(cpt)_2 \cdot 2H_2O]$ (**1**), $[Cu(cpt)(OH) \cdot 2H_2O] \cdot 2H_2O$ (**2**), $[Zn(cpt)_2] \cdot 0.5DMF \cdot CH_3CH_2OH$ (**3**), as well as the reported complex $[Co(cpt)_2 \cdot 2H_2O]$ (**4**) [Hcpt = 4-(4-carboxyphenyl)-1,2,4-triazole and DMF = *N,N*-dimethylformamide]. Complexes **1**, **2**, **3**, and **4** are all obtained under solvothermal conditions. Isomorphous complexes **1** and **4** both display 0D structures, however, complex **4** was already reported.[24] Complex **2** displays 1D chain topology constructed by $Cu(H_2O)_2^{2+}$ cati-

* Dr. J. F. Song
E-Mail: jfsong0129@gmail.com
[a] Department of Chemistry, College of Science
North University of China
Taiyuan, 030051, P. R. China
[b] Shanxi Research Center of Engineering Technology for Engineering Plastics
North University of China
Taiyuan, 030051, P. R. China
Supporting information for this article is available on the WWW under **http://dx.doi.org/10.1002/zaac.201000368** or from the author.

ons, OH^- ions and cpt anions. Complex **3** with large cavity exhibits fourfold interpenetrated diamondoid network topology.

Experimental Section

Materials and Methods

All chemicals and solvents purchased were of reagent grade and used without further purification except Hcpt, which was prepared according to a literature procedure.[26]

Elemental analysis (C, H, N) was performed with a Perkin–Elmer 240C elemental analyzer. IR spectra were measured with a Perkin–Elmer Spectrum One FT–IR spectrometer using KBr pellets. Thermogravimetric analyses (TGA) were performed with a Perkin–Elmer TGA-7000 thermogravimetric analyzer under flowing air at a temperature ramp rate of 10 °C·min^{-1}. The fluorescence spectrum of complex **3** was obtained with a LS 55 florescence/phosphorescence spectrophotometer at room temperature.

Syntheses of Complexes 1–3

[Mn(cpt)$_2$·2H$_2$O] (1): A solution of Hcpt (9.5 mg, 0.05 mmol) in DMF (5 mL) containing triethylamine (28 μL, 2 mmol) was directly mixed with a solution of $MnCl_2·4H_2O$ in water (1 mL, 0.10 mol·L^{-1}) at room temperature in a 15 mL beaker. 3 M HNO_3 was added until the mixture became clear; afterwards, ethanol (2 mL) was added. The resulted colorless solution was transferred and sealed in a 25 mL Teflon-lined stainless steel reactor, and heated at 85 °C for 72 h. Upon cooling to room temperature, the pale pink crystals were filtered and washed with DMF and ethanol. Yield 75 % (based on Hcpt). Elemental analysis $C_{18}H_{16}MnN_6O_6$ (467.31): calcd C 46.22; H 3.42; N 17.98 %; found: C 46.28; H 3.47; N 18.04 %. **IR** (KBr): $\tilde{\nu}$ = (w = weak, m = medium, s = strong) 3169 (m), 2944 (w), 1605 (s), 1535 (s), 1410 (s), 1253 (s), 1095 (s), 1009 (m), 891 (m), 860 (m) 790 (s), 703 (m) cm^{-1}.

[Cu(cpt)(OH)·2H$_2$O]·2H$_2$O (2): The procedure was the same as that for complex **1** except that $MnCl_2·4H_2O$ was replaced by $CuSO_4·5H_2O$ (0.10 mol·L^{-1}). Upon cooling to room temperature, the blue crystals were filtered and washed with DMF and ethanol. Yield 70 % (based on Hcpt). Elemental analysis: $C_9H_{15}CuN_3O_7$ (340.8): calcd. C 31.69; H 4.40; N 12.32 %; found: C 31.75; H 4.50; N 12.37 %. **IR** (KBr): $\tilde{\nu}$ = 3460 (m), 3206 (m), 2947 (w), 1610 (s), 1527 (s), 1413 (s), 1210 (s), 1005 (m), 866 (m) 788 (s), 694 (m) cm^{-1}.

[Zn(cpt)$_2$]·0.5DMF·CH$_3$CH$_2$OH (3): The procedure was the same as that for complex **1** except that $MnCl_2·4H_2O$ was replaced by $ZnCl_2·4H_2O$ (0.10 mol·L^{-1}). Upon cooling to room temperature, the yellow crystals were filtered and washed with DMF and ethanol. Yield 58 % (based on Hcpt). Elemental analysis: $C_{21.50}H_{21.50}N_{6.50}O_{5.50}Zn$ (524.32): calcd. C 49.21; H 4.10; N 14.88 %; found: C 49.25; H 4.09; N 14.92 %. **IR** (KBr): $\tilde{\nu}$ = 3415 (w), 1720 (m), 1602 (s), 1510 (s), 1358 (s), 1068 (m), 739 (s), 628 (m) cm^{-1}.

[Co(cpt)$_2$·2H$_2$O] (4): The procedure was the same as that for complex **1** except that $MnCl_2·4H_2O$ was replaced by $CoCl_2·6H_2O$ (0.10 mol·L^{-1}). Upon cooling to room temperature, the red crystals were filtered and washed with DMF and ethanol. Yield 90 % (based on Hcpt). Elemental analysis: $C_{18}H_{16}CoN_6O_6$ (471.30): calcd. C 45.83; H 3.39; N 17.82 %; found: C 45.85; H 3.45; N 17.84 %. **IR** (KBr): $\tilde{\nu}$ = 3276 (m), 1607 (s), 1539 (s), 1421 (s), 1098 (m), 773 (m), 507 (m) cm^{-1}.

Crystal Structure Determination

The crystal structures were determined by single-crystal X-ray diffraction. The reflection data were collected with a Bruker SMART CCD area-detector diffractometer (Mo-K_α radiation, graphite monochromator) at room temperature with ω-scan mode. Empirical adsorption correction was applied to all data using SADABS program. The structure was solved by direct methods and refined by full-matrix least-squares on F^2 using SHELXTL 97 software.[27] Non-hydrogen atoms were refined anisotropically. Whenever possible, the hydrogen atoms are located on a difference Fourier map and refined. In other cases, the hy-

Table 1. Crystal and structure refinement data for complexes **1**–**3**.

	1	**2**	**3**
Empirical formula	$C_{18}H_{16}MnN_6O_6$	$C_9H_{15}CuN_3O_7$	$C_{21.50}H_{21.50}N_{6.50}O_{5.50}Zn$
Formula weight	467.36	340.78	524.32
Crystal system	Monoclinic	Monoclinic	orthorhombic
Space group	*C*2/*c*	*C*2/*m*	*Pbcn*
a /Å	13.608(3)	26.965(5)	19.7665(9)
b /Å	9.850(2)	6.7463(13)	15.8012(8)
c /Å	14.434(4)	7.1351(14)	16.9680(8)
β /deg	112.529(3).	95.80(3)	
Volume /Å^3	1787.1(7)	1291.3(4)	5299.7(4)
Z	4	4	8
ρ_{calc} /g·cm^{-3}	1.759	1.753	1.314
Absorption	0.795	1.728	0.970
Crystal size /mm	0.25 × 0.20 × 0.15	0.28 × 0.25 × 0.15	0.25 × 0.19 × 0.15
θ range /°	2.63–26.1	3.11–27.47	2.04–25.97
Reflections	4876	6348	27948
Unique [*R*(int)]	1787 (0.0304)	1602 (0.0503)	5201 (0.0742)
Completeness	99.7 %	99.7 %	100.0 %
Goodness-of-fit on F^2	1.037	1.035	1.117
R indexes [$I > 2\sigma(I)$][a)]	R_1 = 0.0380, wR_2 = 0.1138	R_1 = 0.0538, wR_2 = 0.1386	R_1 = 0.0838, wR_2 = 0.2742
R (all data)[a)]	R_1 = 0.0527, wR_2 = 0.1279	R_1 = 0.0697, wR_2 = 0.1520	R_1 = 0.1212, wR_2 = 0.3085

a) $R1 = \Sigma||F_o|-|F_c||/\Sigma|F_o|$; $wR = [\Sigma w(F_o^2-F_c^2)_2/\Sigma w(F_o^2)^2]^{1/2.}$

Zeitschrift für anorganische und allgemeine Chemie ZAAC Journal of Inorganic and General Chemistry

Table 2. Bond lengths /Å and angles /° for complexes **1**–**3**.

1			
Mn(1)–O(1w)	2.143(2)	O(1)–Mn(1)–O(1)#1	117.66(9)
Mn(1)–O(1)	2.205(2)	O(1w)#1–Mn(1)–O(2)	86.00(6)
Mn(1)–O(2)	2.224(2)	O(1w)–Mn(1)–O(2)	86.51(6)
O(1w)#1–Mn(1)–O(1w)	164.2(1)	O(1)–Mn(1)–O(2)	59.50(6)
O(1w)–Mn(1)–O(1)	92.78(6)	O(1)#1–Mn(1)–O(2)	176.72(6)
O(1w)–Mn(1)–O(1)#1	95.41(6)	O(2)–Mn(1)–O(2)#1	123.39(8)
2			
O(1w)–Cu(1)	2.576(4)	O(2)#2–Cu(1)–N(1)	91.47(2)
Cu(1)–O(2)	1.9324(7)	N(1)#2–Cu(1)–N(1)	180.00(1)
Cu(1)–N(1)	2.002(3)	O(2)–Cu(1)–O(1w)	89.98(6)
O(2)–Cu(1)–O(2)#2	180.0(3)	N(1)#2–Cu(1)–O(1w)	90.61(4)
O(2)–Cu(1)–N(1)	88.73(2)	N(1)–Cu(1)–O(1w)	89.59(4)
3			
O(2)–Zn(1)	1.942(5)	O(2)–Zn(1)–N(5)	110.5(2)
O(3)–Zn(1)	1.951(6)	O(3)–Zn(1)–N(5)	102.8(2)
N(2)–Zn(1)	2.040(5)	O2–Zn(1)–N(2)	95.1(2)
N(5)–Zn(1)	2.014(6)	O(3)–Zn(1)–N(2)	112.6(2)
O(2)–Zn(1)–O(3)	130.5(2)	N(5)–Zn(1)–N(2)	102.3(2)

Symmetry transformations used to generate equivalent atoms: #1: $-x$, y, $-z + 1/2$; #2: $-x + 1/2$, $-y + 1/2$, $-z + 1$.

drogen atoms are geometrically fixed in complexes **1**–**3**. The hydrogen atoms of solvents in complexes **2** and **3** are not completely located. The ethanol and disordered DMF molecules in complex **3** are located with Dfix and Isor. All calculations were carried out using SHELXTL 97[27] and PLATON.[28] The crystallographic data and pertinent information are summarized in Table 1. Selected bond lengths and angles are listed in Table 2 and the geometric parameters of hydrogen bonds are listed in Table 3.

Table 3. Hydrogen bonds for complexes **1** and **2**.

D–H···A[a)]	*d*(D–H)	*d*(H···A)	*d*(D···A)	<DHA /°
1				
O1w–H1wB···N2#1	0.776	2.047	2.818	172.80
O1w–H1wA···N1#2	0.973	1.812	2.762	164.48
2				
O1w–H1wA···O1#3	0.835	2.006	2.781	153.96
O1w–-H1wB···O1w#4	0.828	2.153	2.815	136.92
O2w–H2wA···O1#5	0.843	2.044	2.838	156.69
O1···O3w			2.854	
O1···O2w			2.840	

a) D represents "donor" and A represents "acceptor". Symmetry codes: #1: $-x + 1$, y, $-z + 1/2$; #2: $x - 1$, $-y + 1$, $z - 1/2$; #3: $x + 1/2$, $y + 1/2$, z; #4: $-x + 1/2$, $-y + 1/2$, $-z$; #5: $x + 1$, $y + 1$, $z + 1$.

CCDC-796490, CCDC-796491, and CCDC-796492 for complexes **1**–**3**, respectively, contain the supplementary crystallographic data. These data can be obtained free of charge from The Cambridge Crystallographic Data Centre via http://www.ccdc.cam.ac.uk/data_request/cif or from the Cambridge Crystallographic Data Centre, CCDC, 12 Union Road, Cambridge CB2 1EZ, UK (Fax: +44-1223-336-033; or E-Mail: deposit@ccdc.cam.ac.uk).

Supporting Information (see footnote on the first page of this article): IR spectra of complexes **1** and **4** as well as their isomorphous cadmium complex.

Results and Discussion

Synthesis

The ligand Hcpt is insoluble in water or ethanol, however, it is easily solved in DMF, therefore the experiments were carried out under solvothermal conditions. Different metal salts such as $MnCl_2{\cdot}4H_2O$, $CuSO_4{\cdot}5H_2O$, $ZnCl_2{\cdot}4H_2O$, $CoCl_2{\cdot}6H_2O$, $3CdSO_4{\cdot}8H_2O$, or $NiCl_2{\cdot}6H_2O$ were added to Hcpt under mixed DMF/CH_3CH_2OH/H_2O conditions at 85 °C. The 0D complexes containing cobalt, cadmium, or manganese ions were easily obtained, however, the corresponding complexes with higher dimensions were difficult to obtain. The three complexes were confirmed to be isomorphous by infrared spectroscopy (Figure S1) and single-crystal X-ray diffraction. Moreover, the yields may depend on the amount of triethylamine of reaction system, but the reaction was not significantly affected. The highest yields were achieved when the amount of triethylamine is 28 μL. Only unidentified green powders were obtained when cobalt, cadmium, or manganese ions were replaced by Ni^{II} ions. When $MnCl_2{\cdot}4H_2O$ was substituted by $CuSO_4{\cdot}5H_2O$ or $ZnCl_2{\cdot}4H_2O$, complexes **2** or **3** were obtained.

Crystal Structures

*Crystal Structure of Complex **1***

X-ray crystallography reveals that complex **1** with 0D topology structure is isomorphous to the previously reported complexes constructed by the first-transition metal (copper) and cpt anions.[24] Complex **1** is composed of one Mn^{II} ion, two deprotonated cpt anions, and two coordinated water molecules (Figure 1a). The manganese atom with a slightly distorted octahedral arrangement, where the basal plane is occupied by four carboxylate oxygen atoms (O1, O1a, O2, and O2a) from

two chelating cpt⁻ ligands, lies on a crystallographic inversion center, and two symmetry equivalent oxygen atoms of water molecules (O1w and O1wa) in axial positions forms a slightly distorted octahedral arrangement. The axial Mn–O1w bond length [*d*(Mn–O1w) = 2.143(2) Å] is slightly shorter than the equatorial Mn–O bond lengths [*d*(Mn–O1) = 2.205(2) and *d*(Mn–O4) = 2.224(2) Å]. The corresponding bond lengths and angles are listed in Table 2, they further confirm the distorted octahedral arrangement of the manganese atom. In complex **1**, the cpt⁻ coordinates with Mn^{II} in a O,O-chelating mode, however, the nitrogen atoms of the 1,2,4-triazole groups of cpt anions are not coordinated to the metal atoms, similar to the reported coordination mode of cpt⁻.[24]

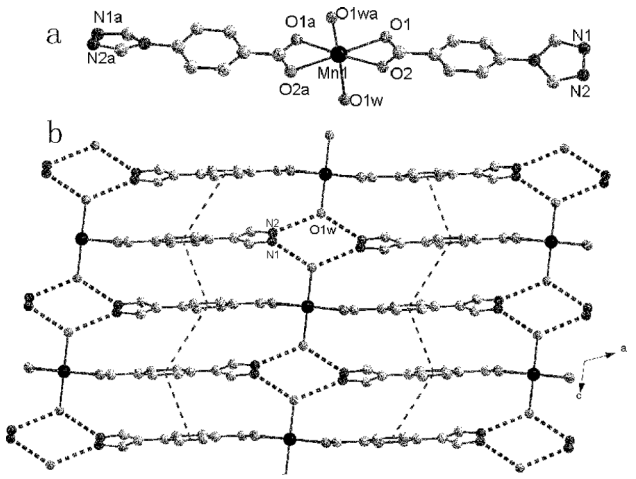

Figure 1. (a) Coordination environment of manganese. (b) 2D supramolecular layer along the *ac* plane constructed by hydrogen bonds in complex **1**. Hydrogen atoms are omitted for clarity.

Each water molecule in complex **1** is involved in two intermolecular O–H···O hydrogen bonds with two uncoordinated nitrogen atoms of the 1,2,4-triazole groups of cpt anions (N1 and N2) from two neighboring molecules to generate a 2D supramolecular structure (Figure 1b), in which two water molecules and two triazole groups form an six-membered ring. The π–π interactions between cpt⁻ stabilize the 2D supramolecular layer (face-to-face distance of 3.4924 Å and offset angle of 11.33°). The corresponding hydrogen bonding parameters are summarized in Table 3.

Crystal Structure of Complex ***2***

The asymmetric unit of complex **2** contains half a Cu^{II} ion, half a μ_2-cpt⁻ anion, half a OH^- ion, a coordinated water and a lattice water molecule. Each copper atom adopts a slightly distorted octahedral arrangement, where the basal plane is occupied by two nitrogen atoms (N1) from two symmetry equivalent cpt⁻ ligands and two oxygen atoms (O2 and O2a) from two symmetry equivalent OH^- anions, and the axial positions are occupied by two symmetry equivalent oxygen atoms from coordinated water molecules (O1w) (Figure 2). Due to Jahn–Teller effect of d^9 configuration, the distance of Cu–O1w (Cu–O1w = 2.536 Å) is longer than the other Cu–O distances. The corresponding bond lengths and angles are listed in Table 2, which further confirms the distorted octahedral arrangement of Cu^{II} in **2**. In **2**, the cpt⁻ ligand coordinates with the Cu^{II} atoms in a μ_2-N,N-bridging mode, which is reported for the first time.

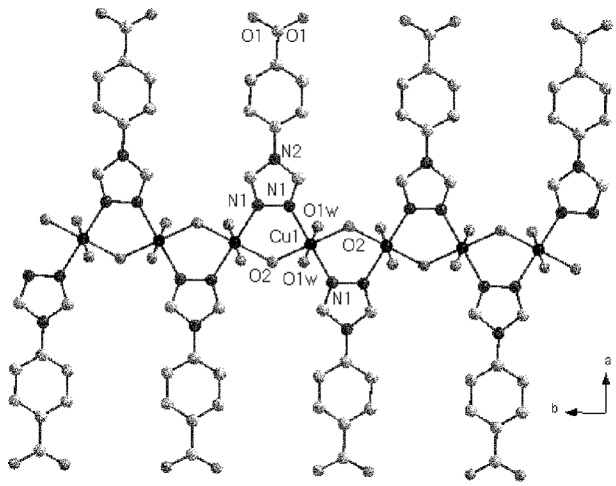

Figure 2. View of the infinite polymeric [Cu(μ-cpt)(μ-OH)] chain in complex **2**.

The copper atoms are joined into an infinite polymeric chain by the μ_2-hydroxo groups together with μ_2-cpt⁻ along the *b* axis (Figure 2). It's noteworthy that the coordinated water molecules (O1w) are interconnected into a 1D water chain through O–H···O hydrogen bonds (O1w–H1wb···O1w) (Figure 3). The 1D water chains and 1D Cu(OH) chains are interconnected into a 2D puckered layer, in which another hydrogen atom (H1wa) is outstretched and acts as hydrogen-bond donor. The 2D layers are joined into a 3D supramolecular network by O1w–H1wa···O1 hydrogen bonds, with two kinds of different oriented channels of dimension 12.67 × 4.46 $Å^2$. Interestingly, O2w and O3w reside in two kinds of different oriented channels, respectively (Figure 4).

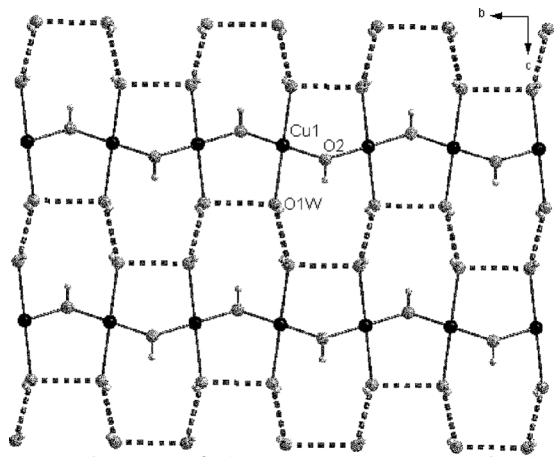

Figure 3. View of the 2D supramolecular puckered layer constructed by 1D water chains and 1D Cu(OH) chains in complex **2**. Cpt⁻ ions are omitted for clarity.

According to the Cambridge Structural Database (release 5.31), we found that dozens of complexes containing the frag-

Zeitschrift für anorganische und allgemeine Chemie ZAAC Journal of Inorganic and General Chemistry

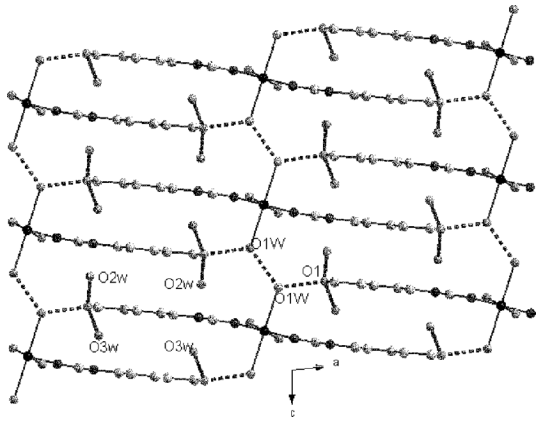

Figure 4. 3D supramolecular network in complex **2**.

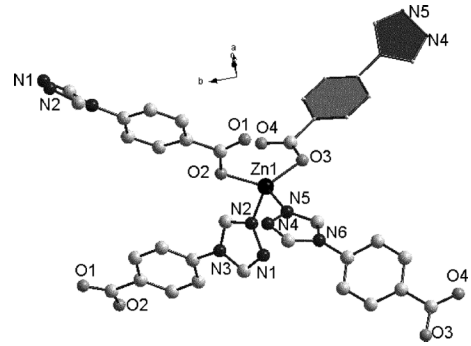

Figure 5. Coordination environment of zinc in complex **3**.

ment [Cu(μ-L)(μ-*X*)] were reported,[29–33] L represents substituted N-containing heterocycle molecules coordinated through the N–N bond in a bidentate bridging manner similarly to **2**, and *X* is a simple bridging group such as OH, F, Cl, I, however, to the best of our knowledge, L, which plays a crucial role in the construction of the fragment [Cu(μ-L)(μ-*X*)], is not an anionic organic ligand but a neutral organic molecule. So, the fragment [Cu(cpt)(OH)] constructed by anionic N-containing heterocycle molecules coordinated by N–N bonds in a bidentate bridging manner was reported for the first time. In addition, compared with the reported similar complex, [Cu(μ-L)(μ-OH)(H_2O)$_2$]·Cl (**5**), the dihedral angle between the benzene ring and the triazole ring in complex **2** is smaller than that of complex **5** (3.01° for complex **2**, and 90.00° for complex **5** [L = 4-(4-hydroxyphenyl)-1,2,4-triazole]).[29]

Crystal Structure of Complex 3

Complex **3** exhibits a 3D open framework with fourfold interpenetrated diamondoid network topology and crystallizes in space group *Pbcn*. The asymmetric unit of complex **3** contains one Zn^{II} ion, two kinds of deprotonated cpt^- anions, one uncoordinated ethanol molecules and half a DMF molecule. Each zinc ion adopts distorted tetrahedral arrangement and is coordinated by two nitrogen atoms (N5 and N2) and two monodentate carboxylate oxygen atoms (O2 and O3) from four μ_2-cpt^- anions (Figure 5). The Zn–O/N bond lengths are in the range 1.942(5)–2.040(5) Å, and the corresponding O/N–Zn–O/N bond angles range from 95.1(2)° to 130.5(2)° (Table 3), which indicate distortion of the zinc tetrahedral arrangement. The difference in the cpt^- anions is the deviation of dihedral angle between the carboxyl plane and the benzene ring or the benzene ring and the triazole ring (the dihedral angle of the carboxyl plane and the benzene ring is 41.34° for cpt^- containing O1, and 40.62° for the other; the dihedral angle of the benzene ring and the triazole ring is 14.22° for cpt^- containing O1, and 1.89° for the other). This difference results from the rotation around the C–C bond among the carboxyl plane, benzene ring and triazole ring.

Different from complexes **1** and **2** as well as the reported complexes based on the ligand Hcpt, cpt^- adopts a new coordination mode in complex **3**: μ_2-N, O-bridging mode. Each Zn^{II} atom is connected by four cpt^- bridging ligands, which consist of two kinds of cpt^-, propagating into a 3D metal-organic framework with diamond topology (Figure 6). The intracage Zn···Zn distances are 13.22 and 12.18 Å, which indicate a significantly large void space of the diamondoid network. In the crystal structure, this void space is filled by a fourfold interpenetration of the diamondoid network and solvent molecules (DMF and ethanol) (Figure 6). The adamantanoid cages are strongly compressed in the interpenetration direction along *b* axis. The interpenetration mode of the four independent nets in complex **3** is the so-called "normal" type for diamondoid frames, which belongs to class *Ia*.[34–38] Interestingly, there exists in a fourfold interpenetration of the diamondoid network in complex **3**, however, very larger void space is still formed. Calculation performed using PLATON reveals a total solvent-accessible volume equal to 2073.6 $Å^3$ per unit cell, which counts for 39.1 % of the cell volume,[28] offering possibilities of gas adsorption and gas separation, etc.

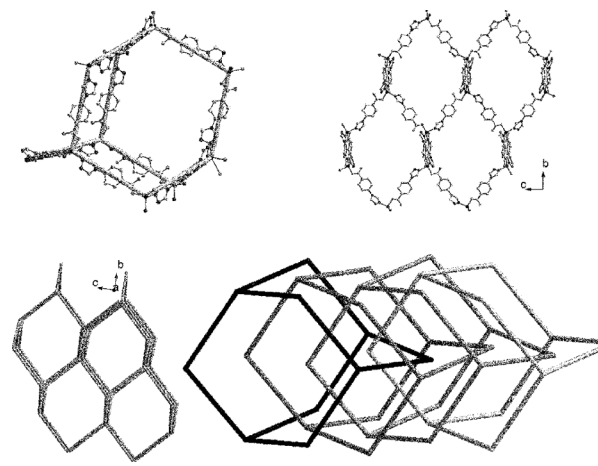

Figure 6. (a) View of a single dia unit cage. (b) A single 3D dia net. (c) Topological representation of a single 3D dia net. (d) Topological representation of the fourfold interpenetrating network of complex **3**.

TG Curves of Complexes 1–3

The thermal behaviors of complexes **1**–**3** were studied from 25 °C to 700 °C in air (Figure 7). The weight loss of complex

1, which occurred at 240 °C, is assigned to the loss of coordinated water. The total weight loss of complex **1** amounts to 82.34 % (calcd. 83.31 %). For complex **2**, the first weight loss 9.73 % occurred in the range 85–142 °C and is attributed to the loss of lattice water. The second weight loss of 65.36 % from 142 °C to 450 °C corresponds to the loss of coordinated water and the decomposition of the organic component. The total weight loss of complex **2** is 75.09 % (calcd. 76.67 %), whereas for complex **3**, the first loss is approximately 22.57 % in the range of 143–316 °C, corresponding to the weight loss of solvent molecules (ethanol and DMF). The second weight loss (58.93 %) occurred between 316 and 530 °C and is characteristic of the combustion of cpt^- ligand. The total weight loss of complex **3** amounts to 81.50 % (calcd. 84.55 %).

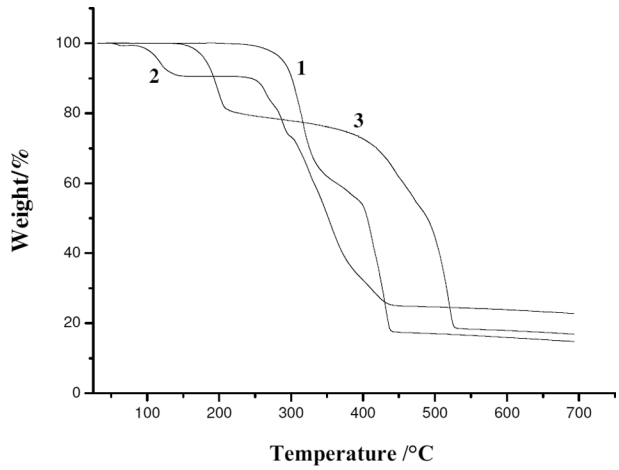

Figure 7. TGA curves of complexes **1**–**3**.

Fluorescence Spectrum of Complex 3

The photoluminescence spectra of complex **3** and the ligand Hcpt in the solid state are shown in Figure 8. Hcpt exhibits blue photoluminescence with an emission maximum at 468 nm upon excitation at 360 nm. Similarly, complex **3** also exhibits blue photoluminescence with an emission maximum at 485 nm upon excitation at 360 nm, respectively. A comparison of the photoluminescence spectra of Hcpt and complex **3** showed that the maximum emission wavelength of complex **3** is similar to that of the ligand Hcpt in terms of position and band shape. Therefore, the emission bands of complex **3** are mainly due to an intraligand emission state similar to the reported d^{10} metal complexes with N-donor carboxylate ligands.[39,40] The intensity increase of the luminescence for these complexes than their corresponding ligands may be attributed to the chelation of the ligand to the metal atom, which increases the rigidity of Hcpt and reduces the nonradiative relaxation process.

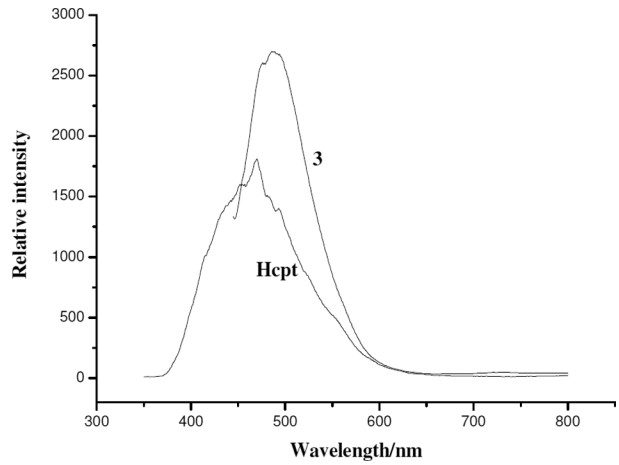

Figure 8. Solid-state emission spectra for complex **3** as well as Hcpt ligand at room temperature.

Conclusions

Three new cpt-Metal complexes displaying 0D, 1D, and 3D topologies were synthesized under solvothermal conditions. Analyses of synthetic conditions, crystal structures and coordination modes of cpt^- revealed that the reaction metal ions have important effects on the structure of these complexes and coordination modes of Hcpt ligand. This study revealed that more new coordination polymers or porous materials with high dimension could be synthesized by using Hcpt. Further research for the construction of new architectures with more transition metals is underway in our laboratory. Complex **3** shows strong blue photoluminescence in the solid state at room temperature.

Acknowledgement

This work was supported by the *Natural Science Young Scholars Foundation of North University of China* and the *Scientific Research Start-up Foundation of North University of China*.

References

[1] M. Eddaoudi, D. B. Moler, H. L. Li, B. L. Chen, T. M. Reineke, M. O'Keeffe, O. M. Yaghi, *Acc. Chem. Res.* **2001**, *s34*, 319.
[2] B. J. Holliday, C. A. Mirkin, *Angew. Chem. Int. Ed.* **2001**, *40*, 2022.
[3] B. Moulton, M. J. Zaworotko, *Chem. Rev.* **2001**, *101*, 1629.
[4] O. M. Yaghi, M. O'Keeffe, N. W. Ockwig, H. K. Chae, M. Eddaoudi, J. Kim, *Nature* **2003**, *423*, 705.
[5] S. Kitagawa, R. Kitaura, S. Noro, *Angew. Chem. Int. Ed.* **2004**, *43*, 2334.
[6] G. Ferey, *Chem. Soc. Rev.* **2008**, *37*, 191.
[7] J. R. Li, R. J. Kuppler, H. C. Zhou, *Chem. Soc. Rev.* **2009**, *38*, 1477.
[8] L. Q. Ma, C. Abney, W. B. Lin, *Chem. Soc. Rev.* **2009**, *38*, 1248.
[9] D. J. Tranchemontagne, J. L. Mendoza-Cortes, M. O'Keeffe, O. M. Yaghi, *Chem. Soc. Rev.* **2009**, *38*, 1257.
[10] W. W. Zhou, J. T. Chen, G. Xu, M. S. Wang, J. P. Zou, X. F. Long, G. J. Wang, G. C. Guo, J. S. Huang, *Chem. Commun.* **2008**, 2762.
[11] M. S. Wang, G. C. Guo, W. Q. Zou, W. W. Zhou, Z. J. Zhang, G. Xu, J. S. Huang, *Angew. Chem. Int. Ed.* **2008**, *47*, 3565.
[12] T. L. Hennigar, D. C. MacQuarrie, P. Losier, R. D. Rogers, M. J. Zaworotko, *Angew. Chem. Int. Ed. Engl.* **1997**, *36*, 972.
[13] A. J. Blake, N. R. Brooks, N. R. Champness, P. A. Cooke, A. M. Deveson, D. Fenske, P. Hubberstey, W. S. Li, M. Schroder, *J. Chem. Soc., Dalton Trans.* **1999**, 2103.

[14] C. Y. Su, Y. P. Cai, C. L. Chen, M. D. Smith, W. Kaim, H. C. Z. Zoye, *J. Am. Chem. Soc.* **2003**, *125*, 8595.
[15] S. C. Chen, Z. H. Zhang, K. L. Huang, Q. Chen, M. Y. He, A. J. Cui, C. Li, Q. Liu, M. Du, *Cryst. Growth Des.* **2008**, *8*, 3437.
[16] B. R. Manzano, F. A. Jalon, M. L. Soriano, M. C. Carrion, M. P. Carranza, K. Mereiter, A. M. Rodriguez, A. de la Hoz, A. Sanchez-Migallon, *Inorg. Chem.* **2008**, *47*, 8957.
[17] T. K. Prasad, M. V. Rajasekharan, *Cryst. Growth Des.* **2008**, *8*, 1346.
[18] G. J. T. Cooper, G. N. Newton, D. L. Long, P. Kogerler, M. H. Rosnes, M. Keller, L. Cronin, *Inorg. Chem.* **2009**, *48*, 1097.
[19] J. C. Liu, G. C. Guo, J. S. Huang, X. Z. You, *Inorg. Chem.* **2003**, *42*, 235.
[20] Y. B. Lu, M. S. Wang, W. W. Zhou, G. Xu, G. C. Guo, J. S. Huang, *Inorg. Chem.* **2008**, *47*, 8935.
[21] R. Vaidhyanathan, S. S. Iremonger, K. W. Dawson, G. K. H. Shimizu, *Chem. Commun.* **2009**, 5230.
[22] J. P. Zhang, X. M. Chen, *J. Am. Chem. Soc.* **2009**, *131*, 5516.
[23] R. Q. Zou, L. Z. Cai, G. C. Guo, *J. Mol. Struct.* **2005**, *737*, 125.
[24] L. V. Lukashuk, A. B. Lysenko, E. B. Rusanov, A. N. Chernega, K. V. Domasevitch, *Acta Crystallogr. Sect. C* **2007**, *63*, m140.
[25] D. Savard, P. H. Lin, T. J. Burchell, L. Korobkov, W. Wernsdorfer, R. Clérac, M. Murugesu, *Inorg. Chem.* **2009**, *48*, 11748.
[26] R. H. Wiley, A. J. Hart, *J. Org. Chem.* **1953**, *18*, 1368.
[27] G. M. Sheldrick, *SHELXS 97*, Program for Crystal Structure Refinement, University of Göttingen: Göttingen, Germany **1998**.
[28] A. L. Spek, *PLATON*, Molecular Geometry Program, University of Utrecht, The Netherlands **1999**.
[29] E. V. Lider, E. V. Peresypkina, A. I. Smolentsev, V. N. Elokhina, T. I. Yaroshenko, A. V. Virovets, V. N. Ikorskii, L. G. Lavrenova, *Polyhedron* **2007**, *26*, 1612.
[30] A. B. Lysenko, E. V. Govor, K. V. Domasevitch, *Inorg. Chim. Acta* **2007**, *360*, 55.
[31] B. Liu, G. C. Guo, J. S. Huang, *J. Solid State Chem.* **2006**, *179*, 3136.
[32] Y. Wang, P. Cheng, Y. Song, D. Z. Liao, S. P. Yan, *Chem. Eur. J.* **2007**, *13*, 8131.
[33] Y. Wang, X. Q. Zhao, W. Shi, P. Cheng, D. Z. Liao, S. P. Yan, *Cryst. Growth Des.* **2009**, *9*, 2137.
[34] I. A. Baburin, V. A. Blatov, L. Carlucci, G. Ciani, D. M. Proserpio, *Cryst. Growth Des.* **2008**, *8*, 519.
[35] http://www.topos.ssu.samara.ru.
[36] V. A. Blatov, L. Carlucci, G. Ciani, D. M. Proserpio, *CrystEngComm* **2004**, *6*, 378.
[37] L. Carlucci, G. Ciani, D. M. Proserpio, S. Rizzato, *CrystEngComm* **2002**, *4*, 413.
[38] S. R. Batten, *CrystEngComm* **2001**, *18*, 1.
[39] S. L. Zheng, J. H. Yang, X. L. Yu, X. M. Chen, W. T. Wong, *Inorg. Chem.* **2004**, *43*, 83.
[40] X. Li, B. L. Wu, C. Y. Niu, Y. Y. Niu, H. Y. Zhang, *Cryst. Growth Des.* **2009**, *9*, 3423.

Received: October 13, 2010
Published Online: December 27, 2010

